émergents" MICRO2). R.M. was supported by an apprentice grant from CNRS. R.M. and E.D. contributed equally to this work. E.D. contributed to the crossing design and the phenotypic analysis. R.M., E.D., M.S., P.M.G., and S.G. contributed to the bioinformatics analysis. E.D., I.F.-L., E.G., and T.G. performed the functional validation experiment. C.P. performed the phylogenetic analysis. M.F. performed the sRNA-seq experiments. E.P., W.M., and H.B. constructed the BAC libraries and performed the screening and BAC sequencing. V.C., S.B., X.V., I.F.-L., and T.G. designed the experiments. All authors discussed the results. E.D., R.M., I.F.-L., X.V., S.B., and V.C. wrote the paper. V.C. and S.B. coordinated the project. *S*-locus sequences have been deposited on the European Molecular Biology Organization public database, sRNA sequences on the GEO public database (see table S2 for accession numbers), and data matrices and phylogenetic trees on the TreeBASE database (http://purl.org/phylo/treebase/phylows/study/TB2:S16394). BAC clones produced in this project will be distributed through http://cnrgv.toulouse.inra.fr/Library/Arabidopsis upon signature of a material transfer agreement for in-house academic research.

SUPPLEMENTARY MATERIALS

www.sciencemag.org/content/346/6214/1200/suppl/DC1
Materials and Methods
Figs. S1 to S12
Tables S1 and S2
References (*39*–*57*)

31 July 2014; accepted 17 October 2014
10.1126/science.1259442

REPORTS

VALLEYTRONICS

Ultrafast generation of pseudo-magnetic field for valley excitons in WSe_2 monolayers

Jonghwan Kim,[1]* Xiaoping Hong,[1]* Chenhao Jin,[1] Su-Fei Shi,[1,2] Chih-Yuan S. Chang,[3] Ming-Hui Chiu,[4] Lain-Jong Li,[3,4] Feng Wang[1,2,5]†

The valley pseudospin is a degree of freedom that emerges in atomically thin two-dimensional transition metal dichalcogenides (MX_2). The capability to manipulate it, in analogy to the control of spin in spintronics, can open up exciting opportunities. Here, we demonstrate that an ultrafast and ultrahigh valley pseudo-magnetic field can be generated by using circularly polarized femtosecond pulses to selectively control the valley degree of freedom in monolayer MX_2. Using ultrafast pump-probe spectroscopy, we observed a pure and valley-selective optical Stark effect in WSe_2 monolayers from the nonresonant pump, resulting in an energy splitting of more than 10 milli–electron volts between the K and K′ valley exciton transitions. Our study opens up the possibility to coherently manipulate the valley polarization for quantum information applications.

Atomically thin layers of transition metal dichalcogenides (MX_2) have emerged as an exciting two-dimensional semiconductor platform for nanoelectronics and optoelectronics (*1*, *2*). In particular, a pair of degenerate bands are present at the K and K′ valleys in the momentum space of hexagonal MX_2 monolayers, giving rise to a valley degree of freedom that is analogous to electron spin (*3*). Recent polarization-resolved photoluminescence (PL) studies show that the valley pseudospin in MX_2 can couple directly to the helicity of excitation photons (*4*–*7*) and that the pseudospin polarization between two valleys exhibits coherent behavior (*7*). It raises the intriguing prospect of valleytronics, which exploits the valley degree of freedom to carry information (*1*, *3*–*9*).

Just as spin manipulation is essential in spintronics, the capability to control the valley pseudospin is essential for valleytronics based on MX_2 materials. In spintronics, the electron spin can be manipulated through any external perturbation that breaks the energy degeneracy of two orthogonal spin polarizations. This can be achieved either through an external magnetic field (*10*, *11*) or through a pseudo-magnetic field generated by other stimuli. For example, circularly polarized light can produce a pseudo-magnetic field that can be used to manipulate electron spins in semiconductor quantum wells and quantum dots (*12*, *13*) through the optical Stark effect. (The optical Stark effect, a well-established phenomenon in atomic physics and quantum optics, describes the energy shift in a two-level system induced by a nonresonant laser field.) It is highly desirable to realize similar control of valley excitons in MX_2 by using light-induced pseudo-magnetic field for valleytronics.

[1]Department of Physics, University of California at Berkeley, Berkeley, CA 94720, USA. [2]Material Science Division, Lawrence Berkeley National Laboratory, Berkeley, CA 94720, USA. [3]Institute of Atomic and Molecular Sciences, Academia Sinica, Taipei 10617, Taiwan. [4]Physical Sciences and Engineering, King Abdullah University of Science and Technology, Thuwal, Saudi Arabia. [5]Kavli Energy NanoSciences Institute, University of California Berkeley and Lawrence Berkeley National Laboratory, Berkeley, CA 94720, USA.
*These authors contributed equally to this work, **†Corresponding author. E-mail: fengwang76@berkeley.edu**

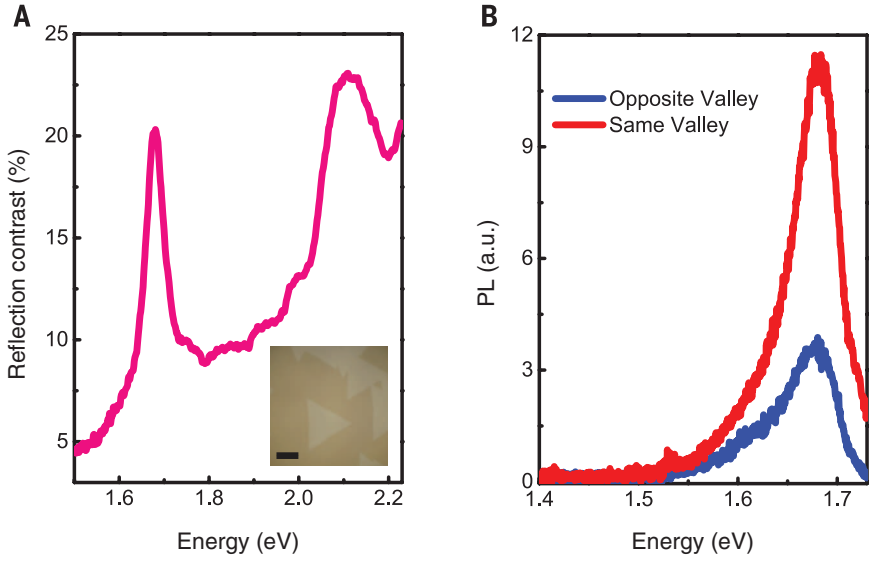

Fig. 1. Valley exciton transitions in monolayer WSe_2. (**A**) The optical reflection spectrum of a WSe_2 monolayer on a sapphire substrate at 77 K. It shows strong A- and B-exciton resonances at 1.68 and 2.1 eV, respectively. (Inset) Optical microscopy image of the sample. Scale bar, 25 μm. (**B**) Polarization-resolved PL spectra of a WSe_2 monolayer at 77K. For a 1.8-eV excitation laser with left circular polarization, the PL spectra show a prominent emission peak at the A-exciton resonance (1.68 eV), and the PL intensity with left circular polarization (red curve) is about four times stronger than that with right circular polarization (blue curve). It demonstrates that valley-polarized A-exciton population can be created by circularly polarized resonant excitation and it can be detected with polarization-resolved PL spectroscopy.

Here, we demonstrate a valley-selective optical Stark effect in monolayer WSe_2 to generate an ultrafast and ultrahigh pseudo-magnetic field for valley excitons. Previously, resonant pump-probe spectroscopy has been used to probe ultrafast carrier dynamics after the pump photons are absorbed by exciton transitions in MX_2 monolayers (*14*–*17*). We used nonresonant circularly polarized laser pumping with photon energies below the bandgap, which induces a coherent and dissipationless valley-selective optical Stark effect for pseudospin manipulation.

We used triangular monolayers of WSe_2 grown by means of chemical vapor deposition on sapphire substrates (Fig. 1A, inset) (*18*). The optical reflection spectrum of monolayer WSe_2 at 77 K exhibits two prominent resonances at 1.68 and 2.1 eV (Fig. 1A), which correspond, respectively, to the A- and B-excitons split by the spin-orbital coupling (*19*, *20*). In this study, we focused on the lowest-energy A-exciton transition. This A-exciton is well separated from other excited states in energy thanks to strong electron-hole interactions in monolayer WSe_2. As a result, we can approximate the ground state and the A-exciton as a two-level system and neglect the effect from other excited states. In monolayer WSe_2, the A-exciton states at K and K′ valleys are time-reversal pairs and have degenerate energy levels. However, they have distinct optical selection rules and couple to photons of opposite helicity (*3*, *4*). The dipole transition matrix element of the K valley A-exciton is characterized by $P_K^{\sigma\pm} = \langle K|\hat{p}_x \pm i\hat{p}_y|0\rangle$, where $|K\rangle$ and $|0\rangle$ correspond to the K valley A-exciton and ground state, respectively; $\hat{p}_x$, $\hat{p}_y$ are momentum operators; and σ_+/σ_- corresponds to left/right circular light. In MX_2 monolayers, $P_K^{\sigma+}$ has a finite value, but $P_K^{\sigma-}$ is approximately zero. Consequently, the A-exciton at the K valley couples exclusively to left-circularly polarized light. The A-exciton at the K′ valley, on the other hand, couples only to the right-circularly polarized light. This dipole selection rule for valley

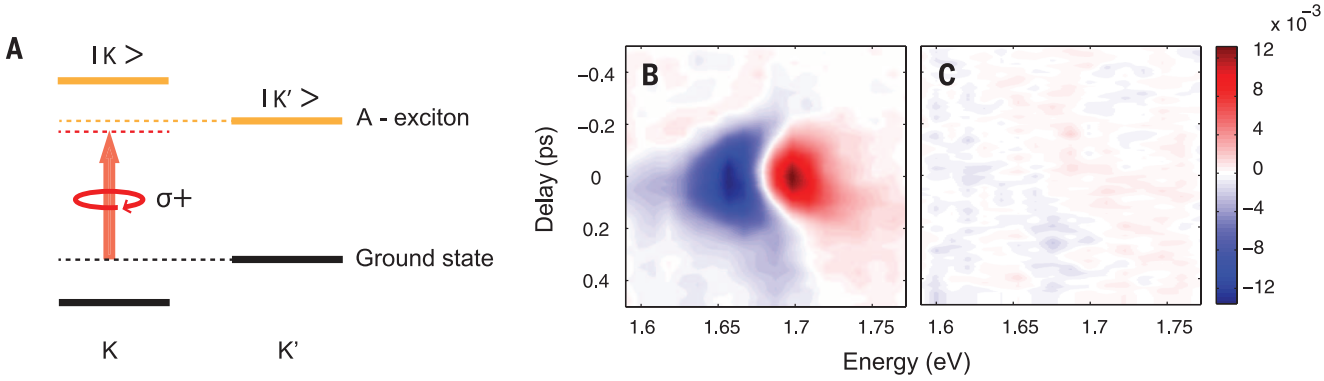

Fig. 2. Valley-dependent optical Stark effect with nonresonant circularly polarized pump. (**A**) Schematic of the optical Stark effect for valley transitions with nonresonant, left circularly polarized σ_+ pump. The dashed black and yellow lines denote the unperturbed ground and exciton states, respectively, and the pump photon energy is lower than the exciton resonance energy (red arrow). In the dressed atom picture, the dressed ground state (with N σ_+ photons) and the K valley A-exciton (with N-1 σ_+ photons) are coupled by dipole transition, which results in energy-level repulsion (left, solid black and yellow lines) and an increased exciton transition energy. On the other hand, σ_+ pump does not affect K′ valley A-exciton resonance because of the optical selection rule (right). (**B** and **C**) Transient reflection spectra of A-exciton resonance at 77 K. The color scale, horizontal axis, and vertical axis represent the relative reflectivity change $\Delta R/R$, the probe photon energy, and the pump-probe time delay, respectively. For atomically thin WSe_2 on sapphire substrate, $\Delta R/R$ is proportional to absorption change. Nonresonant σ_+ pump of photon energy at 1.53 eV leads to (B) a strong transient absorption signal for probes with the same polarization σ_+, but (C) produces no transient response for probes with the opposite polarization σ_-.

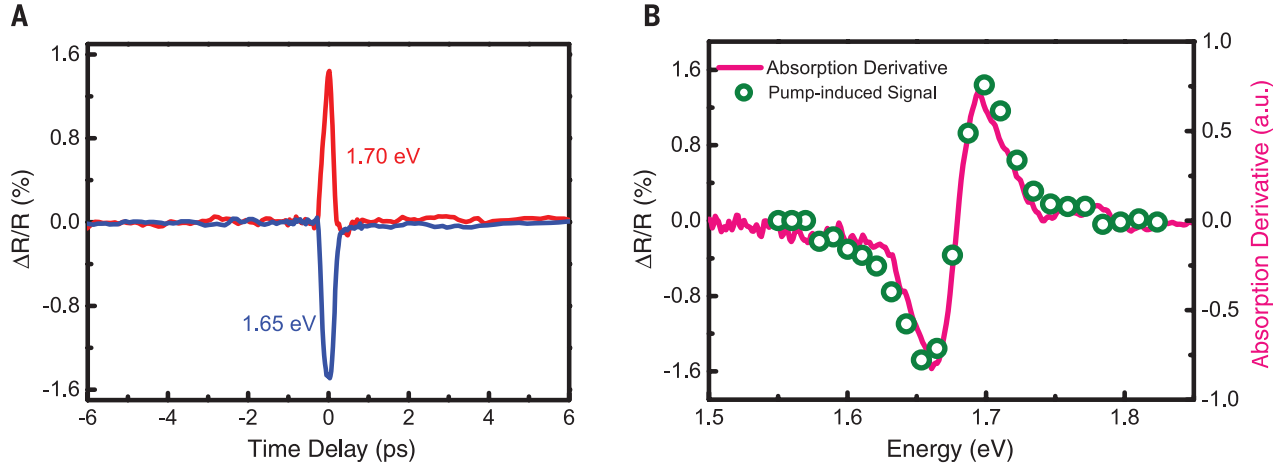

Fig. 3. Time evolution and spectral lineshape of the valley-dependent transient reflection spectra for σ_+ pump and σ_+ probe configuration. (**A**) Time evolution of the pump-induced transient reflectivity $\Delta R/R$ at probe energies of 1.65 eV (blue line) and 1.7 eV (red line). Both signals reach the maximum magnitude at the pump-probe delay $\tau = 0$ with symmetric rise and decay dynamics (limited by our pulse width ~250 fs), which is characteristic of an instantaneous optical response. The transient reflectivity has opposite signs for 1.65 and 1.7 eV probes. (**B**) The transient reflection spectrum at $\tau = 0$ (green circles). The transient reflectivity signal changes sign at the A-exciton resonance energy E_A = 1.68 eV, and it shows a dispersive line shape. This transient reflection spectrum matches well with the derivative of linear absorption spectrum in monolayer WSe_2 and can be fully accounted for by a 4-meV blueshift of the K valley A-exciton resonance (magenta line).

transitions in monolayer WSe_2 governs both resonant and nonresonant excitations, which can have different manifestations in valley physics.

The valley-dependent resonant excitation enables both the generation of a valley-polarized exciton population through the absorption of circularly polarized light and the detection of valley-polarized excitons through polarization-resolved photoluminescence (PL) (*4*–*6*). Displayed in Fig. 1B are polarization-resolved PL spectra of our WSe_2 samples upon laser excitation at 1.8 eV with σ_+ circular polarization, in which the PL intensity with helicity matching the excitation light (σ_+; Fig. 1B, red curve) is about four times stronger than that for the opposite helicity (σ_-; Fig. 1B, blue curve). This behavior is similar to that reported in previous studies (*4*–*7*) and verifies the valley-selective excitation and emission in our WSe_2 monolayers. The nonzero σ_- polarized PL is presumably caused by a finite intervalley scattering because the excitation energy is ~120 meV higher than the A-exciton resonance.

To manipulate the valley polarization, however, nonresonant coupling based on the optical Stark effect is more advantageous because it avoids the dissipation and dephasing naturally accompanying real excitations. The optical Stark effect is widely used in quantum optics to control a rich variety of quantum systems, ranging from the manipulation of cold atoms (*21*) and individual trapped ions (*22*) to coherent control of superconducting qubits (*23*) and electron spins (*24*). In a two-level system, the optical Stark effect can be readily understood by using the dressed-atom picture (*25*). Consider the two-level system composed of the ground state and A-exciton state at the K (or K′) valley in a monolayer WSe_2. Illustrated in Fig. 2A is the effect of a left circularly polarized (σ_+) pump with photon energies below the exciton resonance (Fig. 2A, red arrow). In the dressed-atom picture, the dressed-ground state (with N σ_+ photons), and the K valley A-exciton (with N-1 σ_+ photons) are coupled by the dipole transition, which leads to wave function hybridization and energy-level repulsion. It effectively shifts down the ground-state energy and shifts up the K valley exciton energy. The A-exciton at the K′ valley, on the other hand, cannot couple to the ground state with an extra σ_+ photon because of the optical selection rule, and the related states are not shifted by σ_+ polarized light. As a result, the energy degeneracy between K and K′ valley states is lifted by the valley-selective optical Stark effect, which can be characterized by a valley pseudo-magnetic field.

We measured the valley-selective optical Stark shift in WSe_2 monolayers with nonresonant circularly polarized excitation using pump-probe spectroscopy. Femtosecond pump pulses with tunable photon energies below the A-exciton resonance were generated with an optical parametric amplifier. Optical Stark shifts of the WSe_2 exciton transitions induced by the pump pulses was then probed in transient reflection spectra over the spectral range of 1.59 to 1.77 eV by using a laser-generated supercontinuum light. Displayed in Fig. 2, B and C, are two-dimensional plots of transient reflection spectra in a monolayer WSe_2 with σ_+ and σ_- polarized probe light, respectively, upon σ_+ polarized pump excitation. Here, the nonresonant pump photons are at 1.53 eV, which is 150 meV below the exciton resonance and do not excite any real transitions. The color scale in Fig. 2, B and C, represents the pump-induced change of the probe beam reflectivity $\Delta R/R$, the horizontal axis shows the probe photon energy, and the vertical axis shows the pump-probe time delay. For atomically thin WSe_2 layers on a transparent sapphire substrate, the reflection change $\Delta R/R$ is directly proportional to the change in the absorption coefficient (*26*, *27*). It is apparent that strong changes in the exciton absorption are present only for σ_+ probe pulses (Fig. 2B), and no pump-induced signals can be detected above the noise level for σ_- probe pulses (Fig. 2C). This indicates that the nonresonant σ_+ pump substantially modifies the A-exciton transition at the K valley, but not at the K′ valley.

To better examine the time evolution and spectral lineshape of the photo-induced transient reflection spectra in WSe_2 monolayers, we plot in Fig. 3 vertical and horizontal linecuts of the two-dimensional plot for the σ_+ pump and σ_+ probe configuration (Fig. 2B). Displayed in Fig. 3A are the transient reflection signals at the probe photon energy below (1.65 eV; Fig. 3A, blue line) and above (1.7 eV; Fig. 3A, red line) the exciton resonance at different pump-probe delay τ (Fig. 2B, vertical linecuts). Both signals have the largest magnitude at $\tau = 0$ and show a symmetric rise and decay dynamics. This is characteristic of an instantaneous response, with the rise/decay time limited by the laser pulse width of ~250 fs. It shows that the exciton absorption is modulated only when the pump radiation is present. In addition, the transient reflectivity has opposite signs for probe energies at 1.65 and 1.7 eV. Detailed transient reflection spectrum $\Delta R/R$, which is proportional to the transient absorption change (*26*, *27*), is shown in Fig. 3B (green circles) for $\tau = 0$ through a horizontal linecut in Fig. 2B. We observed that the transient absorption signal changes sign exactly at the A-exciton resonance energy (E_A) = 1.68 eV. The pump laser leads to reduced absorption below E_A and increased absorption above E_A, which matches well the linear derivative of the WSe_2 monolayer absorption spectrum (Fig. 3B, magenta line). Quantitatively, the photo-induced absorption change can be perfectly described by a simple blueshift of ~4 meV of the K valley exciton resonance. The blueshift in transition energy, instantaneous time response, and valley selectivity demonstrate unambiguously the optical Stark effect in monolayer WSe_2 upon nonresonant pump excitation. The photo-induced signal becomes nondetectable immediately after the pump pulses, indicating negligible dissipative processes associated with real exciton absorption. We also performed the pump-probe spectroscopy using linearly polarized pump and probe pulses (fig. S1). Here, photo-induced absorption changes are of similar magnitude, independent of the pump and probe polarizations. This is because the linear-polarized pump has both σ_+ and σ_- components, which lead to optical Stark shifts for both K and K′ valley exciton transitions.

Next, we examined how the valley-selective optical Stark shift varies with the pump laser intensity and detuning. The pump detuning $\hbar\Omega$ is defined as the difference between the exciton resonance energy ($\hbar\omega_0$) and the pump photon energy ($\hbar\omega_p$). Shown in Fig. 4 is the transient reflection data (Fig. 4, left axis) and the corresponding energy shift of the A-exciton energy (Fig. 4, right axis, and supplementary text) at the K valley for σ_+ pump and σ_+ probe configuration with different pump detuning (Fig. 4A, green dots) and pump intensities (Fig. 4B, green dots). We observed that the optical Stark shift is inversely proportional to the pump detuning (Fig. 4A, magenta dashed line) and scales linearly with the laser intensity (Fig. 4B, magenta dashed

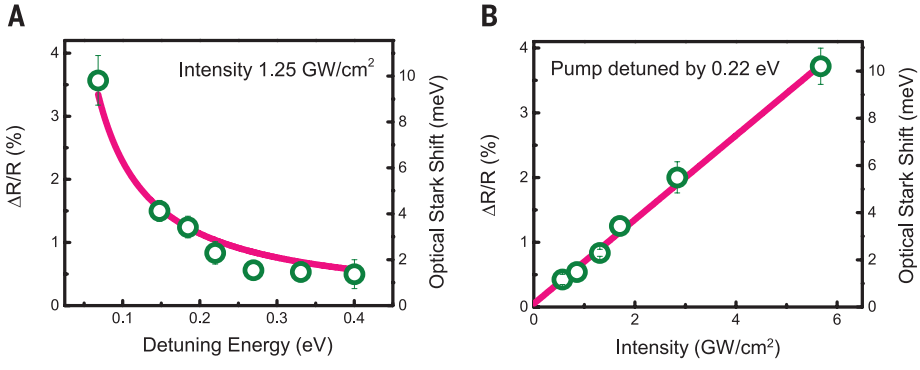

Fig. 4. Pump detuning and pump intensity dependence of the valley-selective optical Stark shift. (**A**) The transient reflection signal at 1.7 eV (left axis) and the corresponding optical Stark shift (right axis) as a function of the pump detuning energy (green dots). The dependence can be nicely described by an inverse proportional relationship (magenta line). (**B**) The transient reflection signal at 1.7 eV (left axis) and the corresponding optical Stark shift (right axis) as a function of the pump laser intensity (green dots), which shows a linear scaling behavior (magenta line). The optical Stark shift can selectively shift the K valley exciton transition by as much as 10 meV, which corresponds to a valley pseudo-magnetic field of ~60 T.

line). Such scaling matches well with the theoretical prediction of optical Stark shift $\delta(\hbar\omega_0) = 2S{\cdot}E_p^2/\hbar\Omega$, where S is the optical Stark shift constant related to the transition dipole moment and E_p is the electric field of the pump pulse (*25*, *28*). From the experimental data, we can determine an optical Stark shift constant $S \sim 45\ D^2$ for A-exciton in monolayer WSe_2, which is of similar magnitude to that for exciton transition in semiconductor quantum wells (*29*).

The valley-selective optical Stark shift breaks the degeneracy of valley exciton transitions in monolayer WSe_2 and defines an effective valley pseudo-magnetic field. In our experiment, the photo-induced energy splitting between K and K′ exciton transitions can be as large as 10 meV (Fig. 4 and supplementary text). The corresponding pseudo-magnetic field B_{eff} for valley excitons can be

estimated with $B_{eff} = \frac{\Delta E}{2g_{ex}\mu_B}$, where μ_B is the Bohr magneton and g_{ex} is the effective g-factor for valley exciton transitions in WSe_2. The effective exciton g-factor g_{ex} combines contributions from both electrons and holes and has a theoretically predicted value of ~1.5 for WSe_2 (supplementary text). Using this g-factor, we estimate a pseudo-magnetic field B_{eff} as high as 60 T for a 10-meV splitting of valley exciton transitions. A real magnetic field of this magnitude is difficult to achieve even with superconducting magnets, but such a pseudo-magnetic field for MX_2 valley excitons can be produced conveniently and with femtosecond temporal control by using light pulses.

It has been reported recently that excitons in different valleys in monolayer WSe_2, resonantly excited by linear polarization light, can maintain their phase coherence over extended time (*7*). The valley-dependent optical Stark effect offers a convenient and ultrafast way to lift the valley degeneracy and introduce a controlled phase difference between the two valley states, therefore enabling coherent rotation of resonantly excited valley polarizations with high fidelity (fig. S2). In analogy with spintronics, such coherent manipulation of valley polarization can open up fascinating opportunities for valleytronics.

REFERENCES AND NOTES

1. X. Xu, W. Yao, D. Xiao, T. F. Heinz, *Nat. Phys.* **10**, 343–350 (2014).
2. Q. H. Wang, K. Kalantar-Zadeh, A. Kis, J. N. Coleman, M. S. Strano, *Nat. Nanotechnol.* **7**, 699–712 (2012).
3. D. Xiao, G. B. Liu, W. Feng, X. Xu, W. Yao, *Phys. Rev. Lett.* **108**, 196802 (2012).
4. T. Cao *et al.*, *Nat. Commun.* **3**, 887 (2012).
5. K. F. Mak, K. He, J. Shan, T. F. Heinz, *Nat. Nanotechnol.* **7**, 494–498 (2012).
6. H. Zeng, J. Dai, W. Yao, D. Xiao, X. Cui, *Nat. Nanotechnol.* **7**, 490–493 (2012).
7. A. M. Jones *et al.*, *Nat. Nanotechnol.* **8**, 634–638 (2013).
8. Y. J. Zhang, T. Oka, R. Suzuki, J. T. Ye, Y. Iwasa, *Science* **344**, 725–728 (2014).
9. K. F. Mak, K. L. McGill, J. Park, P. L. McEuen, *Science* **344**, 1489–1492 (2014).
10. C. P. Poole, *Electron Spin Resonance* (Wiley, New York, ed. 2, 1983)
11. F. H. L. Koppens *et al.*, *Nature* **442**, 766–771 (2006).
12. J. A. Gupta, R. Knobel, N. Samarth, D. D. Awschalom, *Science* **292**, 2458–2461 (2001).
13. D. Press, T. D. Ladd, B. Zhang, Y. Yamamoto, *Nature* **456**, 218–221 (2008).
14. H. Shi *et al.*, *ACS Nano* **7**, 1072–1080 (2013).
15. Q. Wang *et al.*, *ACS Nano* **7**, 11087–11093 (2013).
16. E. J. Sie, Y.-H. Lee, A. J. Frenzel, J. Kong, N. Gedik, Biexciton formation in monolayer MoS2 observed by transient absorption spectroscopy, http://arxiv.org/abs/1312.2918 (2013).
17. C. Mai *et al.*, *Nano Lett.* **14**, 202–206 (2014).
18. J.-K. Huang *et al.*, *ACS Nano* **8**, 923–930 (2014).
19. A. Splendiani *et al.*, *Nano Lett.* **10**, 1271–1275 (2010).
20. K. F. Mak, C. Lee, J. Hone, J. Shan, T. F. Heinz, *Phys. Rev. Lett.* **105**, 136805 (2010).
21. P. Jessen, I. Deutsch, *Adv. At. Mol. Opt. Phys.* **37**, 95–138 (1996).
22. C. Cohen-Tannoudji, *Phys. Scr.* **T76**, 33 (1998).
23. D. I. Schuster *et al.*, *Phys. Rev. Lett.* **94**, 123602 (2005).
24. J. Berezovsky, M. H. Mikkelsen, N. G. Stoltz, L. A. Coldren, D. D. Awschalom, *Science* **320**, 349–352 (2008).
25. C. Cohen-Tannoudji, S. Reynaud, *J. Phys. At. Mol. Opt. Phys.* **10**, 345–363 (1977).
26. F. Wang *et al.*, *Science* **320**, 206–209 (2008).
27. K. F. Mak *et al.*, *Phys. Rev. Lett.* **101**, 196405 (2008).
28. Y.-R. Shen, *The Principles of Nonlinear Optics* (Wiley-Interscience, New York, 1984).
29. A. Von Lehmen, D. S. Chemla, J. E. Zucker, J. P. Heritage, *Opt. Lett.* **11**, 609–611 (1986).

ACKNOWLEDGMENTS

This work was supported by Office of Basic Energy Science, U.S. Department of Energy under contract DE-SC0003949 (Early Career Award) and DE-AC02-05CH11231 (Materials Science Division). L.J.L. thanks the support from Academia Sinica and National Science Council Taiwan (NSC-102-2119-M-001-005-MY3). F.W. also acknowledges the support from a David and Lucile Packard fellowship. All data described in the paper are presented in this report and supplementary materials.

SUPPLEMENTARY MATERIALS

www.sciencemag.org/content/346/6214/1205/suppl/DC1
Materials and Methods
Supplementary Text
Figs. S1 and S2
References (*30*–*34*)

30 June 2014; accepted 5 November 2014
10.1126/science.1258122

HEAVY FERMIONS

Two-dimensional Fermi surfaces in Kondo insulator SmB_6

G. Li,[1] Z. Xiang,[1,2] F. Yu,[1] T. Asaba,[1] B. Lawson,[1] P. Cai,[1,3] C. Tinsman,[1] A. Berkley,[1] S. Wolgast,[1] Y. S. Eo,[1] Dae-Jeong Kim,[4] C. Kurdak,[1] J. W. Allen,[1] K. Sun,[1] X. H. Chen,[2] Y. Y. Wang,[3] Z. Fisk,[4] Lu Li[1]*

In the Kondo insulator samarium hexaboride (SmB_6), strong correlation and band hybridization lead to an insulating gap and a diverging resistance at low temperature. The resistance divergence ends at about 3 kelvin, a behavior that may arise from surface conductance. We used torque magnetometry to resolve the Fermi surface topology in this material. The observed oscillation patterns reveal two Fermi surfaces on the (100) surface plane and one Fermi surface on the (101) surface plane. The measured Fermi surface cross sections scale as the inverse cosine function of the magnetic field tilt angles, which demonstrates the two-dimensional nature of the conducting electronic states of SmB_6.

The recent development of topological insulators is a triumph of single electron band theory (*1*–*8*). Kondo insulators can be used to explore whether similar exotic states of matter can arise in the presence of strong electronic interactions. In these strongly correlated heavy-fermion systems (*9*), the hybridization between itinerant electrons and localized orbitals opens a gap and makes the material insulating. Once the sample temperature is cold enough, the electronic structure can be mapped to a state that resembles a normal topological insulator (TI) (*10*), with a bulk insulating state and a conductive surface state. In samarium hexaboride (SmB_6), the existence of the surface state has been suggested by recent experimental observations of the surface conductance as well as a mapping of the hybridization gap (*11*–*13*). We report the observation of quantum oscillations in Kondo insulator SmB_6 using torque magnetometry via the de Haas–van Alphen (dHvA) effect. The observed Fermi surfaces are shown to be two-dimensional (2D) and arise from the crystalline (101) and (100) surfaces.

One major difference between SmB_6 and the conventional topological insulators is the crystal structure, which for SmB_6 is simple cubic (Fig. 1A). SmB_6 single crystals were grown by conventional flux methods. Each sample was etched with acid to remove the leftover flux. Figure 1B shows a photo of a piece of SmB_6 single crystal. Beside a flat (001) surface, there are four (101) planes.

We use torque magnetometry to resolve the Landau Level quantization and the resulting

[1]Department of Physics, University of Michigan, Ann Arbor, MI 48109, USA. [2]Hefei National Laboratory for Physical Science at Microscale and Department of Physics, University of Science and Technology of China, Hefei Anhui 230026, China. [3]Department of Physics, Tsinghua University, Beijing, China. [4]Department of Physics and Astronomy, University of California at Irvine, Irvine, CA 92697, USA.
***Corresponding author. E-mail: luli@umich.edu**

Ultrafast generation of pseudo-magnetic field for valley excitons in WSe_2 monolayers

Jonghwan Kim *et al.*

Science **346**, 1205 (2014);
DOI: 10.1126/science.1258122

Science (print ISSN 0036-8075; online ISSN 1095-9203) is published weekly, except the last week in December, by the American Association for the Advancement of Science, 1200 New York Avenue NW, Washington, DC 20005.